ORIGINAL ARTICLE

Amie E. Franklin · Inna N. Golubovskaya ·
Hank W. Bass · W. Zacheus Cande

Improper chromosome synapsis is associated with elongated RAD51 structures in the maize *desynaptic2* mutant

Abstract The RecA homolog, RAD51, performs a central role in catalyzing the DNA strand exchange event of meiotic recombination. During meiosis, RAD51 complexes develop on pairing chromosomes and then most disappear upon synapsis. In the maize meiotic mutant *desynaptic2 (dsy2)*, homologous chromosome pairing and recombination are reduced by ~70% in male meiosis. Fluorescent in situ hybridization studies demonstrate that a normal telomere bouquet develops but the pairing of a representative gene locus is still only 25%. Chromosome synapsis is aberrant as exemplified by unsynapsed regions of the chromosomes. In the mutant, we observed unusual RAD51 structures during chromosome pairing. Instead of spherical single and double RAD51 structures, we saw long thin filaments that extended along or around a single chromosome or stretched between two widely separated chromosomes. Mapping with simple sequence repeat (SSR) markers places the *dsy2* gene to near the centromere on chromosome 5, therefore it is not an allele of *rad51*. Thus, the normal *dsy2* gene product is required for both homologous chromosome synapsis and proper RAD51 filament behavior when chromosomes pair.

Introduction

Meiosis couples genetic recombination with the segregation of homologous chromosomes and is broadly con-

A. E. Franklin · I. N. Golubovskaya · W. Z. Cande (✉)
Department of Molecular and Cell Biology,
345 Life Sciences Addition,
University of California at Berkeley,
Berkeley, CA 94720, USA
e-mail: ZCande@uclink4.berkeley.edu

H. W. Bass
Department of Biological Science,
Florida State University,
Tallahassee, FL 32306–4370, USA

served throughout the eukaryotic superkingdom (John 1990). During meiotic prophase, chromosomes identify their homologous partners and undergo homologous recombination. In many organisms, homologous chromosome synapsis is directly preceded by a profound nuclear reorganization, generation of the telomere bouquet (Zickler and Kleckner 1998). Although the telomere bouquet has been postulated to facilitate chromosome association and synapsis by bringing homologous subtelomeric regions into close proximity (Scherthan et al. 1996; Bass et al. 1997), this does not explain how homology is identified between partner chromosomes within the bouquet itself.

During homologous chromosome synapsis, electron microscopy revealed small electron-dense structures between chromosomes that were termed early recombination nodules (RNs) based on their structural similarity to late RNs (reviewed in Zickler and Kleckner 1998). Late RNs have been directly correlated with the occurrence and distribution of chiasmata and meiotic recombination events (Carpenter 1975). Though the role of early RNs is still subject to debate, they were predicted to contain recombination enzymes and be involved in a subclass of recombination events, namely gene conversion (Carpenter 1987). The relationship between these early RNs and recombination-type events has been confirmed, in part, by immunoelectron microscopy. Anderson et al (1997) and Tarsounas et al. (1999) have demonstrated the presence of RecA homologs (described below) associating specifically with early RNs in lily and in mice. However, it is an open question as to whether or not these early RNs are converted into late RNs.

Genetic studies in budding yeast have demonstrated that the eukaryotic RecA homologs, RAD51 and DMC1, are involved in meiotic recombination (Bishop et al. 1992; Shinohara et al. 1992). Meiotic recombination is initiated by the introduction of a double-stranded break by the protein SPO11 (Keeney et al. 1997). Single-stranded 3′ DNA tails are created by other proteins, and RAD51 and DMC1 are then loaded onto these 3′ single-stranded DNAs where they act to mediate recombination (Rock-

mill et al. 1995). In vitro, RAD51 protein can polymerize onto single-stranded DNA and the resulting nucleoprotein filament can undergo DNA strand invasion into a homologous double-stranded DNA target (Baumann et al. 1996), so it makes sense that RAD51 is involved in identification of homologous sequences.

The relationship between recombination and homologous synapsis is unclear since some organisms require SPO11 for synapsis, and others do not. For example, in mice, it has been demonstrated that SPO11-induced double-stranded breaks (monitored by a unique histone phosphorylation) and the subsequent recruitment of RAD51/DMC1 to these sites occurs prior to the initiation of synapsis (Mahadevaiah et al. 2001). In other organisms, such as *Caenorhabditis elegans* (Dernberg et al. 1998) and *Drosophila* (McKim and Hayashi-Hagihara 1998), SPO11 is dispensable for homologous chromosome synapsis but is still required for meiotic recombination. Thus, we cannot generalize about the relationship between homologous synapsis and recombination. However, there may be a relationship between recombination and homologous pairing. In mice and maize, while chromosomes are pairing in zygotene, numerous RAD51 foci are present on the unpaired and paired chromosomes, suggesting that some recombination machinery components may be involved in homolog recognition (Ashley et al. 1995; Franklin et al. 1999).

We have been investigating RAD51 behavior in situ by utilizing three-dimensional immunofluorescence microscopy. By preserving both nuclear and chromosome structure, we have been able to visualize the subnuclear distribution and morphology of native RAD51 complexes in maize meiotic nuclei (Franklin et al. 1999). Maize (*Zea mays*, L.) undergoes chiasmate meiosis and shares many features of meiotic chromosome behavior in common with humans and mice. In maize, single and double RAD51 foci appear on the chromosomes maximally (range 100–700 foci per nucleus) during zygotene when chromosomes are pairing. When chromosomes are completely aligned and synapsed during pachytene, the number of RAD51 foci, i.e. approximately 2–3 per chromosome, is similar to the number of expected reciprocal exchanges between homologs. Based on these patterns of RAD51 distribution, it is possible that RAD51 is involved in two sequential processes during meiosis, namely the search for homology during chromosome pairing and then the actual process of meiotic recombination itself.

We have undertaken genetic and cytological analysis of the maize *desynaptic2* meiotic mutant, previously identified during a screen for meiotic mutants (Golubovskaya and Mashnenkov 1976; Golubovskaya 1989). The mutant phenotype is first obvious at the zygotene stage when chromosomes associate and synapse in maize male meiosis. Fluorescent in situ hybridization demonstrated that a normal telomere bouquet develops but the pairing of the 5S rDNA locus is still reduced to 25% of normal. Immunolocalization of RAD51 during zygotene revealed thin elongated RAD51 structures along or around a single chromosome or stretched between two chromosomes. In contrast, normal maize RAD51 zygotene structures are present as small single and double spheres on chromosomes. Therefore, the normal *dsy2* gene product is required for homologous chromosome synapsis and the normal pattern of RAD51 distribution during zygotene.

Materials and methods

Genetic mapping

Genetic mapping of the *dsy2* gene was performed using *waxy*-linked translocation chromosomes and translocation B chromosomes. For simple sequence repeat (SSR) segregation analysis, the *dsy2* mutant (parental inbred line A344) was outcrossed to the W23 inbred line and selfed. The tissue samples were collected from 12 F2 *dsy2* mutants, and parental W23 and A344 individuals. Polymorphisms between W23 and A344 inbred lines were identified for chromosome 5 SSR markers p-bnlg1208, located in bin 5.03, p-dupssr10, located in bin 5.04, and p-bnlg1346, located in bin 5.07 (see the maize database at http://www.agron.missouri.edu/ssr.html for publicly available sequence data for these primers). DNA purification and the polymerase chain reaction (PCR) were performed essentially according to the SSR Method Manual, also at http://www.agron.missouri.edu/ssr.html. The PCR samples were electrophoresed on a 5% polyacrylamide/TAE gel and stained with ethidium bromide to visualize bands.

Light and electron microscopy

For light microscopy a squash technique was used to determine chiasmata frequency and number of bivalents per male metaphase I cell in three genotypes: *dsy2/dsy2* homozygous mutants (four plants); *dsy2/+* fertile heterozygous sib plants (two plants); and +/+ parental A344 inbred line plants (two plants). Young tassels with anthers in meiotic stages prophase I through tetrads were fixed in freshly mixed Farmer's solution for 24 h at room temperature. The fixed material was then rinsed three times and stored in 70% ethanol at 4°C. Anthers at the diakinesis/metaphase I stages were stained with 2% acetocarmine (Carmine, C1022, Sigma) and chromosomes analyzed by light microscopy. The rod-shaped bivalents indicative of a single chiasma were clearly distinguishable from the ring-shaped bivalents, which typically contain two or more chiasmata (Golubovskaya 1994).

For the analysis of female meiosis, young ears of four *dsy2* mutant plants were fixed according to Golubovskaya and Avalkina (1994), and stained with Feulgen's Reagent. A total of 119 ovules at different meiotic stages were examined.

A spreading technique was used for examination of maize synaptonemal complexes (SCs) in spermatocytes by transmission electron microscopy. Fresh anthers with meiocytes in prophase I stages were identified by light microscopy and used for preparing a suspension of meiocytes. Suspensions of whole nuclei were spread on the surface of 0.2 M sucrose solution, fixed by exposure to the vapor of 37% formalin (Formaldehyde no. F1635, Sigma) for 1–4 h, dried for 2–3 days at room temperature and stained with 50%–70% silver nitrate (Silver Nitrate S-0139, Sigma) according to the protocol of Gillies (1981).

Fluorescent in situ hybridization

Digoxigenin-labeled DNA probe for the 5S rDNA locus was generated by PCR as follows. A 325 bp BamHI repeat of the 5S rDNA locus was subcloned into the BamHI site of Bluescript plasmid (Stratagene) and flanking T3 and T7 primers were used to amplify the insert. Telomere fluorescent in situ hybridization

(FISH) was performed as described (Bass et al. 1997). Fixation of the tissue and hybridization of the probe was performed as described (Bass et al. 1997) except for the following modifications. The anthers were only fixed for 45 min and after FISH and washes, the polyacrylamide anther pads were incubated in antibody blocking solution (Boehringer Mannheim) for 1 h followed by overnight incubation in blocking solution containing FAB fragments of anti-digoxigenin antibodies coupled to horseradish peroxidase. After 1 day of washes (1 h each; 1×PBS, 0.5% Tween 20, 0.1% NP40), the pads were incubated with fluorescein isothiocyanate-TSA reagent for 5 min followed by another hour of washing. The slides were then stained with 4′,6-diamidino-2-phenylindole and mounted.

Immunofluorescence and microscopy

Analysis of RAD51 protein levels during meiosis in *dsy2* mutants and their normal siblings was performed by immunoblotting as described previously (Franklin et al. 1999). Staining for RAD51 and three-dimensional deconvolution microscopy were performed on anthers in meiotic prophase as described (Franklin et al. 1999). Criteria for staging was based on nuclear volume and extent of chromosome compaction, which was not altered significantly in *dsy2* mutants as compared with their normal siblings. Computer modeling was performed on leptotene (*n* =5), pachytene (*n* =6), and 3 of the 6 zygotene nuclei. For nuclear modeling, each RAD51 structure was identified and given an *x*, *y*, *z* coordinate and then its structure classified as single (spherical focus), double focus/bar, filament (long thin) or complex (everything else).

Results

To understand better homologous chromosome pairing, we evaluated several features of chromosome behavior in the maize chromosome pairing mutant *desynaptic2*. This mutant appears to be partially deficient in homology recognition and forms abnormal RAD51 structures during chromosome pairing. Further, this analysis supports an involvement of RAD51 complexes in homologous chromosome synapsis.

Improper synapsis occurs in the *dsy2* mutant

Electron microscopy of silver-stained SC spreads was performed to determine whether or not the *dsy2* mutant has these structures and to characterize the level of synapsis in male meiosis. Unfortunately, it was very difficult to obtain good spreads of *dsy2* mutant SCs, compared with the relative ease of obtaining SC spreads of wild-type sibs and other meiotic mutants (data not shown). As a result only a few nuclei were studied. This suggests that SC formation in *dsy2* nuclei may be more transitory, less complete, or the structure somehow "less sturdy" than normal.

As shown in Fig. 1A, the mutant does have synaptonemal axial and lateral elements (synapsed axial elements). The regions of apparently normal synapsis of the SC exhibit normal spacing between the lateral elements 136±8 nm (*n* =42), which is similar to that measured for a wild-type sibling, 141±14 nm (*n* =98). There are regions of improper chromosome synapsis, mostly incomplete
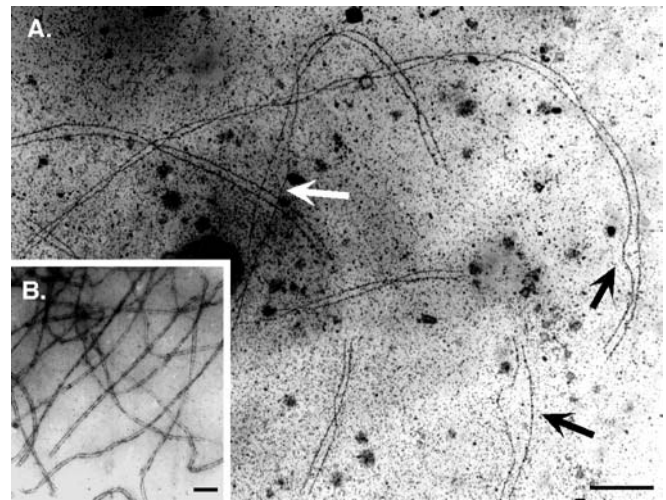

Fig. 1A, B Synapsis in the *dsy2* mutant and normal nuclei. Electron microscopy of silver-stained synaptonemal complexes (SCs) from a *dsy2* mutant (**A**) and from its wild-type sibling (**B**). An unsynapsed but co-aligned region in the *dsy2* mutant (*white arrowhead* in **A**). Two large unsynapsed bulges with lateral elements mismatched in length (*black arrowheads* in **A**). Regular homologous synapsis of SC set in wild-type sibling (**B**). *Bars* in **A** and **B** represent 1 μm

synapsis both in interstitial and terminal chromosome regions, as can be seen by the "bulges". In Fig. 1A, the white arrow points to one of these bulges, which is too wide for synapsis. The two black arrows both point to asymmetric loops of the SC. Again the lateral elements are too far apart to synapse properly. In the spreads of *dsy2* prophase I nuclei that we analyzed, neither switching of chromosome partners nor foldbacks indicating nonhomologous synapsis were found. In contrast, an SC spread from a wild-type *dsy2* sibling, shown in Fig. 1B, has perfectly co-aligned lateral elements that are synapsed throughout their whole length. Thus, the presence of synapsed chromosomes in the mutant indicates that the pathway of synapsis, either proximity-dependent and/or homology-dependent synapsis, is present, but complete synapsis is not achieved.

Homologous pairing is reduced in the *dsy2* mutants

To determine the percentage of synapsed chromosomes that were homologously synapsed, we used FISH to monitor the extent of homologous pairing at the 5S rDNA locus by the pachytene-diplotene stages when homologous pairing, synapsis and recombination are normally complete. Analysis of *dsy2* mutant cells revealed that this locus was paired only 25% of the time at pachytene-diplotene (*n* =120, data not shown). For comparison, pairing at this locus at the same stage in wild-type cells is 100% (Golubovskaya et al. 2002).

The telomere bouquet is normal in *dsy2* mutants

One of the important events immediately preceding chromosome pairing is the formation of the telomere bouquet (Zickler and Kleckner 1998). We performed FISH to monitor the behavior of telomeres in the mutant to determine whether this structure, or lack thereof, could account for the mutant phenotype. This revealed that *dsy2* mutants do develop a telomere bouquet during the zygotene pairing stage (Fig. 2A–C). Nevertheless, the presence of a normal telomere bouquet was insufficient to lead to normal chromosome pairing later on.

Recombination is reduced in male
and female *dsy2* meiocytes

The formation of chiasmata is coupled with crossing over (Creighton and McClintock 1931; Stern 1931). Analysis of acetocarmine-stained male meiocytes at diakinesis and metaphase I allowed us to count the total number of univalents versus rod (one crossover) and ring (two crossovers) bivalent chromosomes. In both wild-type siblings of *dsy2* mutants and the parental inbred line A344, the expected complement of ten ring bivalents is formed nearly all of the time during male meiosis (Table 1, Fig. 3A). This is consistent with the expected number of 25 total crossovers (Darlington 1934). In contrast, during male meiosis in the mutant, most chromosomes were present as univalents. However, the presence of three rod bivalents, on average, in many mutant nuclei indicates that recombination can occur, albeit at an almost tenfold reduced level (Table 1, Fig. 3B–D).

Chiasmata formation during female meiosis in *dsy2* mutants also was reduced; however, this reduction was not as severe as that observed for male meiosis (Fig. 3E–I). Of a total of 38 cells evaluated at diakinesis/metaphase I, 21 cells had the expected number of ten bivalents whereas the remaining 17 cells had fewer bivalents, ranging from two to eight bivalents. For example, 11 chromosomes are evident in Fig. 3E, indicating the
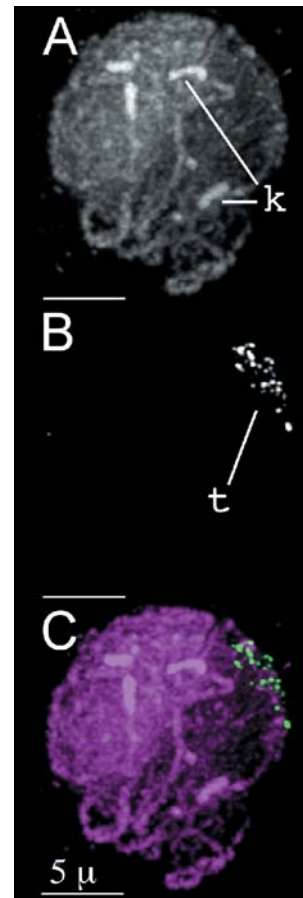

Fig. 2A–C Telomere bouquet develops in *dsy* 2 mutants. Projections of a zygotene nucleus stained with the DNA dye (*white*) 4′, 6-diamidino-2-phenylindole (DAPI) (**A**), counterstained with the telomere fluorescent in situ hybridization (FISH) probe (*white*) (**B**) and the merged image of DNA (*purple*) and telomeres (*green*) (**C**). The heterochromatic DNA structures called knobs (*k*) are unpaired in **A**. In **B** *t* points to the telomere bouquet in which all the telomeres are clustered together on the nuclear envelope. All *bars* represent 5 μm

Table 1 Pattern of recombinant chromosomes in male meiosis. Acetocarmine-stained metaphase I microsporocyte cells were analyzed and the number of bivalent chromosomes and number of chiasmata were determined for *dsy2* mutants (*dsy2* mut), their wild-type siblings (*Dsy2* wt), and their wild-type inbred parental line A344 (A344 wt). The number of cells containing 0–10 bivalents is presented, and the percentage of the total is shown in parenthesis. The total number of cells and average number of bivalents for each genotype are presented. The number of chiasmata in each cell was also determined (a univalent has 0, a rod bivalent has 1, and a ring bivalent has 2) but only the mean number of chiasmata per bivalent is presented

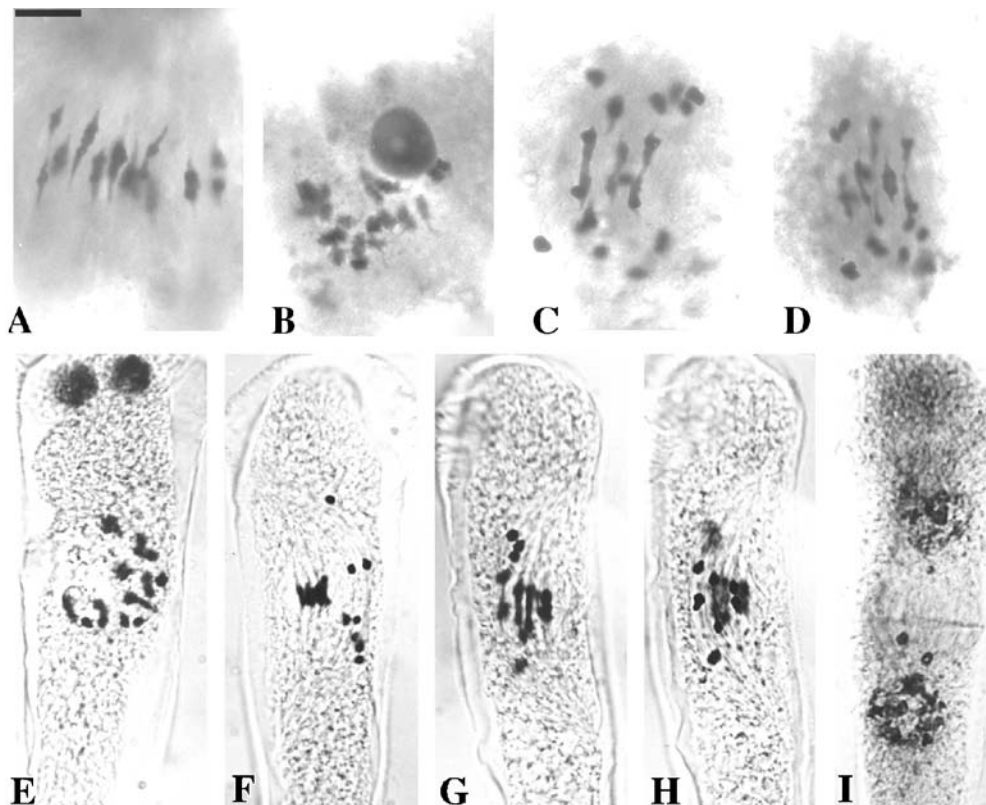| Cell type	Number of bivalents per cell											Total no. cells	Average no. bivalents (mean±SE)	No. chiasmata per bivalent (mean±SE)
	0	1	2	3	4	5	6	7	8	9	10			
dsy2 mut	28 (14%)	25 (12%)	50 (24%)	46 (22%)	31 (15%)	21 (10%)	5 (2%)	0	0	1 (0.5%)	0	207	2.56±0.114	1.07±0.131
Dsy2 wt	0	0	0	0	0	0	1 (1%)	0	5 (3%)	25 (14%)	152 (83%)	183	9.79±0.040	1.79±0.131
A344 wt	0	0	0	0	0	0	0	0	1 (1%)	2 (3%)	74 (96%)	77	9.95±0.031	(1.92±0.125

Fig. 3A–I Chromosome segregation in normal and *dsy2* mutant male and female meiosis. Acetocarmine-stained metaphase I spreads of normal male meiosis (**A**), in *dsy2* mutant male meiosis (**B–D**), and in *dsy2* mutant female meiosis (**E–I**). The normal complement in maize meiosis of ten bivalents (eight ring-shaped, each with at least two chiasmata, and two rod-shaped bivalents, each with one chiasmata) is apparent in **A** with chromosomes beginning to separate at the metaphase-anaphase I stage. Ten univalents and five open bivalents are seen in *dsy2* male meiosis at diakinesis (**B**). Two metaphase I cells are shown (**C, D**): three open rod-shaped bivalents plus 14 univalents are shown in the first cell and five bivalents (four rod-shaped and one ring-shaped) plus ten univalents are seen in the second cell. The presence of both univalents and many rod-shaped one-chiasmata bivalents at diakinesis-metaphase I of *dsy2* demonstrates a severe decrease in chiasmata formation in male meiosis of the mutants. Univalents are prematurely distributed to the spindle poles at metaphase I (**C, D**). At diakinesis in *dsy2* female meiosis (**E**) most chromosomes, with the exception of one pair, are present as bivalents (five rod-shaped and four ring-shaped). Bivalents (mostly ring-shaped) are aligned at the metaphase plate and univalents are at the spindle poles (**F, G, H**). Different optical sections of the same megaspore mother cell are displayed to demonstrate better the univalents (**G, H**). Finally, a telophase I cell has numerous micronuclei (**I**). All images of female meiocytes are cropped at the bottom. *Bar* represents 5 μm

presence of nine recombined bivalents and two univalents. The higher level of chiasmata in female versus male *dsy2* meiocytes probably indicates a higher level of successful pairing and recombination during female meiosis.

dsy2 is not a *rad51* gene since these genes are located on different chromosomes

In many different organisms, RAD51 complexes decorate chromosomes as they are pairing and synapsing, suggesting an involvement of these complexes in the pairing process (Ashley et al. 1995; Franklin et al. 1999; Tarsounas et al. 1999). In *dsy2* mutants, chromosomes do not synapse properly, resulting in a significant reduction in the number of recombined bivalent chromosomes. Could the lesion be in the *rad51* genes? Genetic

mapping of the *dsy2* gene was performed to compare its location with the locations of the two known *rad51* genes (for details see Materials and methods). Genetic repulsion of *dsy2* was observed for chromosome 5 (*waxy*-linked) translocation chromosomes. However, plants hypoploid for a chromosome 5 translocation B chromosome (missing one copy of either the short or long arm of a normal chromosome 5) failed to exhibit the *dsy2* phenotype even though previous genetic data suggested that the *dsy2* mutation is located on chromosome 5. Since the *dsy2* mutant phenotype was not uncovered by hypoploidy of either the short or long arm chromosome 5 translocations, despite the mutation's repulsion to chromosome 5, these data together suggest that the *dsy2* gene is located near the centromere of chromosome 5. To confirm this position, linkage analysis of SSRs located on chromosome 5 to the *dsy2* mutation was performed on a segregating F2 population (see Materials and methods). The *dsy2* mutant
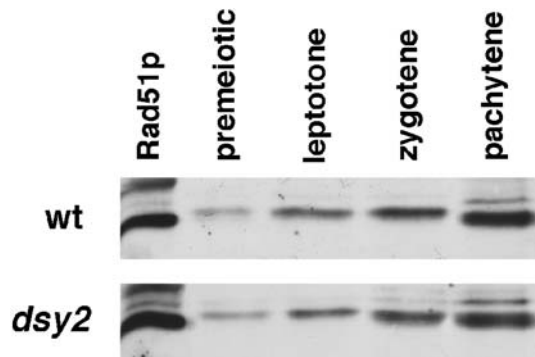
Fig. 4 RAD51 protein accumulates to normal levels in *dsy2* mutants. Immunoblot analysis of staged meiotic anther extracts (three anthers per lane) from wild type (*wt, top row*) and *dsy2* mutants (*bottom row*). *Lane 1* bacterially expressed maize RAD51A protein (1 ng), *lane 2* premeiotic anthers, *lane 3* leptotene anthers, *lane 4* zygotene anthers, *lane 5* pachytene anthers

phenotype co-segregated 100% of the time with the parental SSR markers at 5.03 and 5.04 (*n*=12, data not shown), which are adjacent to the centromeric region of chromosome 5. Independent assortment occurred between the *dsy2* mutant and the SSR marker at 5.07, which is on the long arm of chromosome 5. These data indicate that *dsy2* is located at or near the centromere of chromosome 5 in bin 5.04. A mutation in either *rad51a* or *rad51b*, which are located on chromosomes 7 and 3, respectively (Franklin et al. 1999), cannot explain the *dsy2* phenotype.

Elongated RAD51 structures are present on synapsing chromosomes

To determine whether *dsy2* mutants have reduced RAD51 levels, protein gel immunoblot analysis of staged meiotic anthers was performed. Normal levels of RAD51 protein were observed in the mutant as compared with a normal sib from a segregating family (Fig. 4) ruling out a *trans* effect by the *dsy2* mutation on RAD51 protein accumulation during meiosis.

Another possibility is that RAD51 is not localized properly within the cell. To address this question, we performed three-dimensional immunofluorescence on *dsy2* male meiocytes using anti-RAD51 antiserum as described previously (Franklin et al. 1999). The immunofluorescence revealed that RAD51 complexes do form on the chromosomes during the zygotene and pachytene stages, thereby indicating that the timing of RAD51 recruitment to chromosomes is normal (Fig. 5). However, there was a remarkable difference in the shape of the RAD51 complexes in the mutant relative to wild type only during the zygotene stage. In the mutants we mostly observed highly elongated RAD51 structures of approximately 0.5 to 3 μm in length (Figs. 5E, H, 6) whereas normal cells primarily contain either single RAD51 foci approximately 0.25 μm in diameter or double-contiguous RAD51 foci on the chromosomes (Franklin et al. 1999).
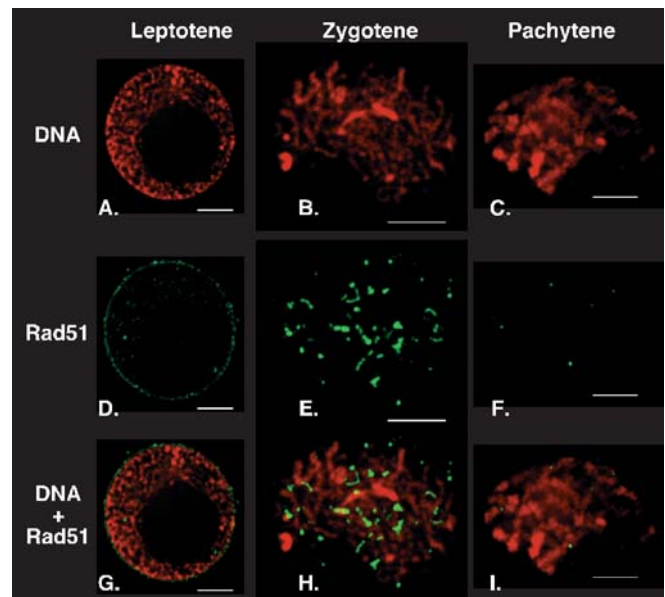

Fig. 5A–I RAD51 structures during meiosis in *dsy2* mutants. Partial projections of one-third of *dsy2* nuclei in leptotene (**A**, **D**, **G**), zygotene (**B**, **E**, **H**), and pachytene (**C**, **F**, **I**) stages stained with the DNA dye DAPI (*red*) (**A**, **B**, **C**), and immunostained for RAD51 (*green*) (**D**, **E**, **F**), and merged images of DAPI and RAD51 staining (**G**, **H**, **I**). In leptotene, RAD51 staining is mostly perinuclear or diffuse within the nucleus (**D**, **G**). By zygotene, many large thread-like and globular RAD51 structures can be seen associated with chromosomes or spanning between unpaired chromosomes (**E**, **H**). In pachytene, these large RAD51 structures are mostly gone; instead there are only a couple of single spherical RAD51 foci (**F**, **I**). All *bars* represent 1 μm

The total numbers of RAD51 structures per nucleus during the zygotene stage were reduced in the mutants relative to wild-type nuclei (~125 vs ~500) despite the equivalent amount of RAD51 protein in the meiotic anthers. However, because individual RAD51 structures in the mutant were significantly larger than those in wild-type zygotene nuclei, the total amount of polymerized RAD51 protein may be similar in the mutant and wild-type meiocytes, consistent with the observation that RAD51 protein levels are similar in wild-type and mutant meiocytes.

Quantification and modeling of RAD51 complexes in *dsy2* mutant nuclei confirmed the apparently normal behavior of RAD51 during the leptotene and pachytene stages and its unusual behavior/structure in the zygotene stage. Leptotene nuclei contained on average 8±4 weak, single spherical RAD51 foci (range 5–14, *n* =5), which is similar to that observed previously for wild-type maize (Franklin et al. 1999). Pachytene nuclei usually contained a few single spherical RAD51 foci, typically 8–11 per nucleus, (range 0–32). The higher number observed in one nucleus may represent a late zygotene nucleus since we cannot readily discriminate between late zygotene and early pachytene stages in *dsy2*. In this nucleus, 13 of the 32 RAD51 structures were long and thin and not spherical. As described above, the RAD51 structures in
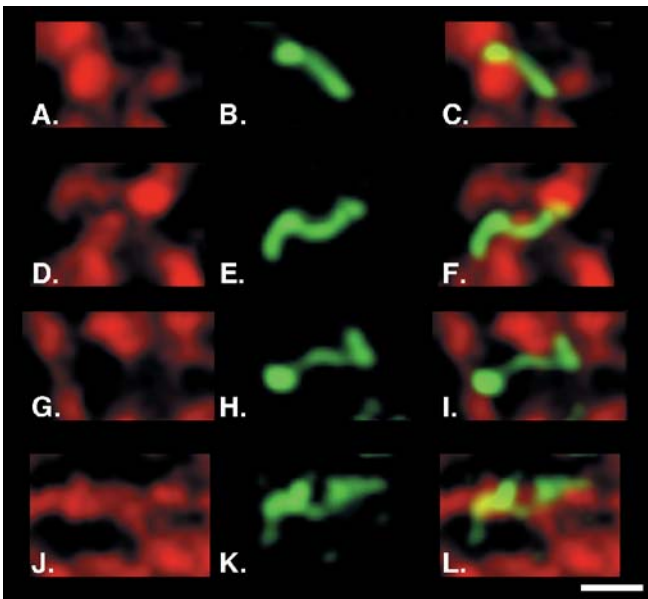
Fig. 6A–L Details of RAD51 structures during zygotene in *dsy2* mutants. Projections (6–10 focal planes equivalent to 1.8–3.0 μm depth) of individual DNA-RAD51 structures computationally extracted from the three-dimensional data sets of zygotene *dsy2* mutant nuclei. Stained as described in Fig. 3: DNA dye (*red*) (**A**, **D**, **G**, **J**), RAD51 (*green*) (**B**, **E**, **H**, **K**) and merged images (**C**, **F**, **I**, **L**). All images scaled identically; *bar* represents 1 μm

the mutant zygotene nuclei were a variety of shapes and the total number of structures ranged from 109–148 per nucleus (three of six nuclei were modeled). Despite the presence of unusual RAD51 structures, ~44% (range 39%–51%) of the structures were single spherical RAD51 foci. This is in contrast to normal zygotene nuclei where ~70% of RAD51 structures are present as single foci. The remaining RAD51 structures in *dsy2* nuclei, accounting for 56% of the total structures, were categorized as double foci/bar RAD51 structures (~13%; range 9%–19%), long filaments (~25%; range 20%–33%), and complex RAD51 structures (~18%; range 15%–20%) This later category included everything that could not be easily defined, e.g. multi-V shapes, wrap-around a chromosome, multi-arm structures. The higher proportion of large/long RAD51 structures in the mutant, ~56% versus the ~30% double foci, dumbbell-shaped structures in wild-type cells, may reflect RAD51 dynamics that are faster in normal versus mutant cells, possibly due to efficient coupling of homologous pairing with synapsis leading to disappearance of RAD51 structures (Plug et al. 1998). Many of the RAD51 filaments are quite long: one nucleus contained 12 filaments over 1 μm in length with the longest at 2.9 μm.

The RAD51 structures presented in Fig. 6 are representative of the aberrant RAD51 structures in mutant zygotene nuclei. The image in Fig. 6C displays an asymmetric RAD51 filament slightly longer than 1 μm. In Fig. 6F the curve in the filament occurs when it traverses the chromosome, suggesting that it is lying along the

surface of the chromosome. In Fig. 6I the RAD51 structure exhibits two bright anchor points both on the chromosomes with a thinner filament spanning the interchromosomal space. In Fig. 6L, the RAD51 structure on the surface of the chromosome is more complex with small finger-like branches emanating from a mass of RAD51 staining.

Discussion

Characterization of the maize meiotic mutant *desynaptic2* by FISH, electron microscopy, and immunofluorescence microscopy reveals that the mutants fails to undergo normal levels of homologous chromosome pairing and synapsis. Aberrant synapsis of chromosomes in male meiosis was demonstrated by electron microscopy of silver-stained SCs showing regions of normal synapsis interspersed by large bulges in the SCs. Pairing of a representative genetic locus, the 5S rDNA locus, occurred 25% of the time at pachytene, compared with 100% in wild type. This level of pairing is very similar to the reduction in number of bivalents seen in male metaphase spreads: two to three bivalents typically observed out of a possible ten expected. Analysis by FISH revealed that *dsy2* mutants have a normal telomere bouquet, in contrast to *pam1* mutants, which show an aberrant bouquet (Golubovskaya et al. 2002), and *desynaptic1* mutants, which show a telomere misplacement phenotype (Bass et al. 2003). This rules out an abnormal bouquet as the cause of aberrant pairing. Instead, the presence of unusual RAD51 structures on the chromosomes during the pairing stage of zygotene suggests that these may be involved in the improper chromosome pairing. Often, highly elongated RAD51 filaments appear to meander through the internuclear space. These may be a direct manifestation of failure in the search for chromosomal homology.

Electron microscopy analysis of *dsy2* demonstrates axial elements that are capable of synapsing at normal spacing, but the presence of bulges is a clear indication of missynapsis. However, electron microscopy data alone cannot demonstrate whether synapsis is homologous or nonhomologous since synapsis can proceed via either a homology-dependent or a proximity-dependent process. Since the pairing of the 5S rDNA locus only occurred ~25% of the time then, by inference, there may be a significant level of nonhomologous synapsis in the mutant. Nevertheless, this level of pairing still indicates that there is some successful homology search occurring since it is higher than what would be expected from random association. For example, if chromosome arms were synapsing at random without regard to any homology in the mutant, then we would expect a subtelomeric locus such as the 5S rDNA locus to pair properly only 2.6% of the time (1/39) since there are 40 subtelomeric arms (2 n=20) in the telomere bouquet. Since homologous pairing is nearly ten times higher than this random level, this suggests that the pathway of homologous pairing is present but much less efficient.

The interpretation that homologous pairing is inefficient in *dsy2* is supported by the difference observed in the number of recombinant chromosomes at metaphase I between male and female meiosis in the *dsy2* mutant. In female meiosis, the expected ten bivalents (n=10) were observed over 50% of the time, whereas this was never observed for male meiosis. Meiosis starts nearly 2 weeks earlier in ovules (female meiosis) as compared with anthers (male meiosis) and proceeds over a longer period of time, which may allow the homologs enough time to find their correct partner. Consequently, despite the presence of an inefficient homologous pairing pathway in *dsy2*, there may be enough time to compensate for this loss of efficiency in female meiosis.

Since pairing and recombination were reduced in *dsy2*, we determined whether or not RAD51 may be responsible for this phenotype. By mapping *dsy2* genetically to the centromeric region of chromosome 5, we ruled out a direct mutation in either of the two known *rad51a* or *rad51b* genes. Next, we performed protein blot analysis on staged anthers and determined that *dsy2* mutants have an equivalent amount of RAD51 protein to wild type, ruling out the possibility of a lack of RAD51 protein. However, immunofluorescence analysis of RAD51 revealed that RAD51 structures in mutants are very unusual during zygotene when chromosomes pair and synapse. Despite overall lower numbers of RAD51 structures, ~125 in the mutant versus ~500 in wild type, there is the same amount of RAD51 protein in mutant anthers and conceivably a similar amount of polymerized RAD51 protein, resulting in significantly larger/longer RAD51 structures.

The RAD51 structures present in *dsy2* may represent exaggerations of normal RAD51 structures and give a hint as to how a normal RAD51 structure develops during chromosome pairing. Aberrant RAD51 structures in the mutant are characterized by the presence of one bright end that appears to be anchored to a chromosome followed by a long finger-like projection extending along or across to another chromosome (Fig. 6) Sometimes, the mutant filaments were wrapped around chromosomes; at other times they traversed across long (0.7 μm) interchromosomal spaces as if they were blindly searching for a partner chromosome. In contrast, normal RAD51 structures in maize are either single or comma-shaped foci or double-contiguous foci that span the space across the SC (~0.2 μm; Franklin et al. 1999). This suggests that RAD51 structures in general may develop by polymerizing first on one chromosome and then growing unidirectionally from it toward another chromosome. This is consistent with the molecular analysis of Holliday junctions, demonstrating the presence of a new structural intermediate termed the single end invasion (Hunter and Kleckner 2001). In the case of *dsy2*, we suggest that a DNA strand coated with RAD51 is formed on one chromosome and initiates its local search for another chromosome, but in many cases, never identifies its homologous chromosome and persists inappropriately.

What could be the normal function of *desynaptic2* protein? Since RAD51 complexes form on chromosomes and there is still some meiotic recombination, we think it is unlikely that DSY2 is involved in double-strand break formation like SPO11. More likely, the DSY2 protein may be a part of the RAD51 complex and is required to regulate its function. If RAD51 polymerization occurs in an uncontrolled fashion, the RAD51 filament may continue to grow even when another chromosome is in close proximity. Alternatively, DSY2 protein may have only an indirect effect on RAD51 in the pairing process. For example, *dsy2* may be a mutation in an SC protein. In the mutant the SC may be unable to serve as a scaffold to guide RAD51 to a homologous chromosome. In the absence of a guide RAD51 would grow out at random instead of growing directly toward an adjacent chromosome. Even with no direction, the RAD51 structure will have a low but significant chance of accidentally bumping into the right chromosome owing to the alignment of chromosome arms in the telomere bouquet. The function of DSY2 should be clarified upon cloning of its gene.

In *dsy2*, aberrant RAD51 structures are present at the time when chromosomes are not properly pairing, suggesting a causal involvement. However, recombination is also reduced in the mutant. Allers and Lichten (2001) have demonstrated that two different types of recombination outcomes, noncrossover (or gene conversion) events and crossover events, are formed at different times during meiosis. Noncrossover events are formed earlier than crossover events. It has been hypothesized that noncrossover/gene conversion events are an outcome of the chromosome homology search mediated by enzymes associated with early RNs such as RAD51 and DMC1 (Carpenter 1987). In the light of this hypothesis, the data could be interpreted as follows: aberrant RAD51 structures in *dsy2* are attempting but unable to perform efficiently a homology search (a noncrossover event) to mediate chromosome pairing, and the reduction in recombination (a crossover event) in the mutant is a secondary consequence of the general failure in homologous chromosome synapsis.

Disentangling the relationship of RAD51 to recombination and homologous chromosome pairing has been difficult. A nearly universal observation has been the unexpectedly high number of RAD51 foci during the early stages of meiosis when chromosomes are undergoing pairing and synapsis (e.g. Terasawa et al. 1995; Franklin et al. 1999). The numbers of foci are orders of magnitude larger than the expected number of recombination events for plants and animals. Furthermore, many foci are observed on unsynapsed chromosomes and on chromosome regions that do not undergo recombination, such as the unpaired regions of the X and Y chromosomes (Ashley et al. 1995). To accommodate these observations RAD51 may be performing another role during zygotene, separate from its role in meiotic recombination. The data presented here are consistent with this proposal as is the phenotype of the *dmc1* mouse knockout (Yoshida et al. 1998) in which chromosomes synapse promiscuously,

suggesting that RecA homologs, RAD51 and DMC1, may be required for ensuring homologous synapsis through a homology sensing function.

References

Allers T, Lichten M (2001) Differential timing and control of noncrossover and crossover recombination during meiosis. Cell 106:47–57

Anderson LK, Offenberg HH, Verkuijlen WMHC, Heyting C (1997) RecA-like proteins are components of early meiotic nodules in lily. Proc Natl Acad Sci USA 94:6868–6873

Ashley T, Plug AW, Xu J, Solari AJ, Reddy G, Golub EI, Ward DC (1995) Dynamic changes in Rad51 distribution on chromatin during meiosis in male and female vertebrates. Chromosoma 104:19–28

Bass HW, Marshall WF, Sedat JW, Agard DA, Cande WZ (1997) Telomeres cluster de novo before the initiation of synapsis: a three-dimensional spatial analysis of telomere positions before and during meiotic prophase. J Cell Biol 137:5–18

Bass HW, Bordoli SJ, Foss EM (2003) The desynaptic (dy) and the desynaptic1 (dsy1) mutations in maize (*Zea mays* L.) cause distinct telomere-misplacement phenotypes during meiotic prophase. J Exp Bot 54:39–46

Baumann P, Benson FE, West SC (1996) Human Rad51 protein promotes ATP-dependent homologous pairing and strand transfer reactions in vitro. Cell 87:757–766

Bishop DK, Park D, Xu L, Kleckner N (1992) DMC1: a meiosis-specific yeast homolog of *E. coli* recA required for recombination, synaptonemal complex formation, and cell cycle progression. Cell 69:439–456

Carpenter ATC (1975) Electron microscopy of meiosis in *Drosophila melanogaster* females. II: The recombination nodule—a recombination associated structure at pachytene? Proc Natl Acad Sci USA 72:3186–3189

Carpenter ATC (1987) Gene conversion, recombination nodules, and the initiation of meiotic synapsis. Bioessays 6:232–236

Creighton HB, McClintock B (1931) A correlation of cytological and genetical crossing over in *Zea mays*. Proc Natl Acad Sci USA 17:492–497

Darlington CD (1934) The origin and behavior of chiasmata. VII. *Zea mays*. Z Indukt Abstammungs Vererbungsl 67:96–114

Dernberg AF, McDonald K, Moulder G, Barstead R, Dresser M, Villanueve A (1998) Meiotic recombination in *C. elegans* initiates by a conserved mechanism and is dispensible for homologous chromosome synapsis. Cell 94:387–398

Franklin AE, McElver J, Sunjevaric I, Rothstein R, Bowen B, Cande WZ (1999) Three-dimensional microscopy of the Rad51 recombination protein during meiotic prophase. Plant Cell 11:809–824

Gillies CB (1981) Electron microscopy of spread maize pachytene synaptonemal complexes. Chromosoma 83:575–591

Golubovskaya IN (1989) Meiosis in maize: mei-genes and conception of genetic control of meiosis. Adv Genet 26:149–192

Golubovskaya IN (1994) A smear technique for the study of meiosis in pollen mother cells. In: Freeling M, Walbot V (eds) The maize handbook. Springer, Berlin Heidelberg New York, pp 447–449

Golubovskaya IN, Avalkina NA (1994) Protocol for preparing maize macrospore mother cells for the study of female meiosis and embryo-sac development. In: Freeling M, Walbot V (eds) The maize handbook. Springer, Berlin Heidelberg New York, pp 450–454

Golubovskaya IN, Mashnenkov AS (1976) Genetic control of meiosis: II. A desynaptic mutant in maize induced by N-nitroso-N-methylurea. Genetika 12:7–14 (in Russian)

Golubovskaya IN, Harper L, Pawlowski WP, Schichnes D, Cande WZ (2002) The pam1 gene is required for meiotic bouquet formation and efficient homologous synapsis in maize (*Zea mays*, L.) Genetics 162:1979–1993

Hunter N, Kleckner N (2001) The single-end invasion: an asymmetric intermediate at the double-strand break to double-holliday junction transition of meiotic recombination. Cell:106 59–70

John B (1990) Meiosis. Cambridge University Press, New York

Keeney S, Giroux CN, Kleckner N (1997) Meiosis-specific DNA double-strand breaks are catalyzed by Spo11, a member of a widely conserved protein family. Cell 88:375–384

Mahadevaiah SK, Turner JM, Baudat F, Rogakou EP, de Boer P, Blanco-Rodriguez J, Jasin M, Keeney S, Bonner WM, Burgoyne PS (2001) Recombinational DNA double-strand breaks in mice precede synapsis. Nat Genet 27:271–276

McKim KS, Hayashi-Hagihara A (1998) mei-W68 in *Drosophila melanogaster* encodes a Spo11 homolog: evidence that the mechanism for initiating meiotic recombination is conserved. Genes Dev 12:2932–2942

Plug AW, Peters AH, Keegan KS, Hoekstra MF, de Boer P, Ashley T (1998) Changes in protein composition of meiotic nodules during mammalian meiosis. J Cell Sci 111:413–423

Rockmill B, Sym M, Scherthan H, Roeder GS (1995) Roles for two RecA homologs in promoting meiotic chromosome synapsis. Genes Dev 9:2684–2695

Scherthan H, Weich S, Schwegler H, Heyting C, Haerle M, Cremer T (1996) Centromere and telomere movements during early meiotic prophase of mouse and man are associated with the onset of chromosome pairing. J Cell Biol 134:1109–1125

Shinohara A, Ogawa H, Ogawa T (1992) Rad51 protein involved in repair and recombination in *Saccharomyces cerevisiae* is a RecA-like protein. Cell 69:457–470

Stern C (1931) Zytologisch-genetische untersuchungen als beweise fur die Morgansche theorie des faktoraustauschs. Biol Zentbl 51:547–587

Tarsounas M, Morita T, Pearlman RE, Moens PB (1999) RAD51 and DMC1 form mixed complexes associated with mouse meiotic chromosome cores and synaptonemal complexes. J Cell Biol:147 207–220

Terasawa M, Shinohara A, Hotta Y, Ogawa H, Ogawa T (1995) Localization of RecA-like recombination proteins on chromosomes of the lily at various meiotic stages. Genes Dev 9:925–934

Yoshida K, Kondoh G, Matsuda Y, Habu T, Nishimune Y, Morita T (1998) The mouse RecA-like gene Dmc1 is required for homologous chromosome synapsis during meiosis. Mol Cell 1:707–718

Zickler D, Kleckner N (1998) The leptotene-zygotene transition of meiosis. Annu Rev Genet 32:619–697